C–H Activation

International Edition: DOI: 10.1002/anie.201508540
German Edition: DOI: 10.1002/ange.201508540

Binuclear Aromatic C–H Bond Activation at a Dirhenium Site

Richard D. Adams, Vitaly Rassolov,* and Yuen Onn Wong*

Abstract: *The electronically unsaturated dirhenium complex $[Re_2(CO)_8(\mu\text{-}H)(\mu\text{-}Ph)]$ (**1**) has been found to exhibit aromatic C–H activation upon reaction with N,N-diethylaniline, naphthalene, and even [D_6]benzene to yield the compounds $[Re_2(CO)_8(\mu\text{-}H)(\mu\text{-}\eta^1\text{-}NEt_2C_6H_4)]$ (**2**), $[Re_2(CO)_8(\mu\text{-}H)(\mu\text{-}\eta^2\text{-}1,2\text{-}C_{10}H_7)]$ (**3**), and [D_6]-**1**, respectively, in good yields. The mechanism has been elucidated by using DFT computational analyses, and involves a binuclear C–H bond-activation process.*

The activation of C–H bonds is a critical step in the transformation of saturated hydrocarbons into new higher-value products.[1,2] Low-valent metal atoms in complexes have been found to be very effective agents for performing C–H bond cleavage.[1–4] Examples involving activation of aromatic C–H bonds by polynuclear metal complexes are rare.[5]

In recent studies, we discovered a facile C–H bond-forming process leading to benzene formation by the NCMe-induced reductive elimination of the bridging phenyl ligand and the bridging hydrido ligand from the complex $[Re_2(CO)_8(\mu\text{-}H)(\mu\text{-}\eta^1\text{-}C_6H_5)]$ (**1**) to yield the complex $[Re_2(CO)_8(NCMe)_2]$ [Equation (1).][6]

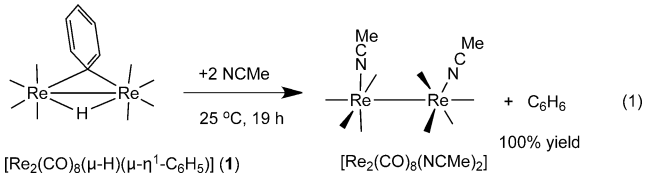

(1)

We have now found that **1** is equally capable of performing facile activation of aromatic C–H bonds and can be used as a reagent for the formation of new dirhenium complexes containing bridging aryl and bridging hydrido ligands. The reaction of **1** with *N,N*-diethylaniline yielded benzene and the new dirhenium complex $[Re_2(CO)_8(\mu\text{-}H)(\mu\text{-}\eta^1\text{-}C_6H_4NEt_2)]$ (**2**) in 61% yield after 5.5 hours at 50 °C [Equation (2)].

An ORTEP diagram of the molecular structure of **2** as determined by single-crystal X-ray diffraction analysis is shown in Figure 1. The structure of **2** is similar to that of **1** and contains a bridging hydrido ligand and C-coordinated

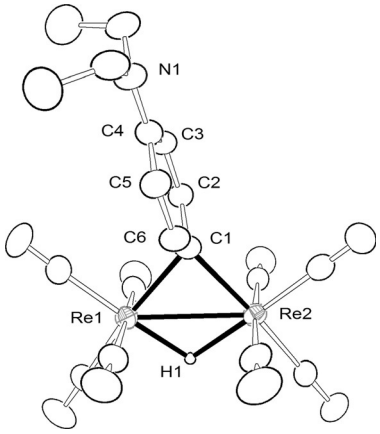

Figure 1. An ORTEP diagram of the molecular structure of $[Re_2(CO)_8(\mu\text{-}\eta^1\text{-}C_6H_4NEt_2)(\mu\text{-}H)]$ (**2**). Thermal ellipsoids shown at 30% probability. Selected interatomic bond distances (Å) are as follows: Re1–Re2 = 2.9720(4) Å, Re1–C1 = 2.338(5), Re2–C1 = 2.269(4), Re1–H1 = 1.77(4), Re2–H1 = 1.86(4).

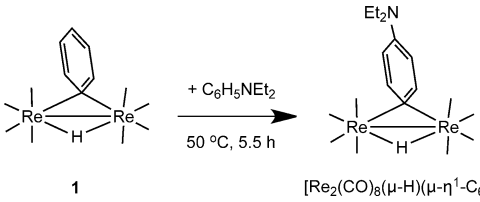

(2)

η^1-bridging $C_6H_4NEt_2$ ligand. The NEt_2 group lies *para* to the coordinated carbon atom. As in **1** the Re–Re bond distance is short, 2.9720(4) Å, because of electronic unsaturation at the metal atoms (32 valence electrons for **2** versus the expected 34 electron configuration). The Re–C distances to the bridging $NEt_2C_6H_4$ ligand are slightly different, Re1–C1 = 2.338(5) Å and Re2–C1 = 2.269(4) Å. A similar asymmetry was also observed in **1**.[6] A single hydride ligand, H1 ($\delta = -11.96$ ppm), bridges the Re–Re bond on the side opposite to the $C_6H_4NEt_2$ ligand.

The compound **1** was also found to react with naphthalene to yield the new compound $[Re_2(CO)_8(\mu\text{-}H)(\mu\text{-}\eta^2\text{-}1,2\text{-}C_{10}H_7)]$ (**3**) in 44% yield within 15 hours at 50 °C. An ORTEP diagram of the molecular structure of **3** is shown in Figure 2. The compound **3** contains two rhenium atoms, a bridging hydrido ligand and an η^2-bridging (σ-π coordinated) $C_{10}H_7$ (naphthyl) ligand. The naphthyl ligand was formed by the elimination of benzene from **1** and the oxidative addition of naphthalene at a C–H bond at the 2-position. The carbon atom C1 is bonded to both Re atoms: Re1–C1 = 2.433(4) Å and Re2–C1 = 2.196(4) Å while C2 is bonded only to Re1, Re1–C2 = 2.599(4) Å. One hydrido ligand also bridges the Re–Re bond ($\delta = -12.82$ ppm).

[*] Dr. R. D. Adams, Dr. V. Rassolov, Dr. Y. O. Wong
Department of Chemistry and Biochemistry
University of South Carolina
JM Palms Ctr for GSR, Columbia, SC 29208 (USA)
E-mail: ADAMSRD@mailbox.sc.edu
RASSOLOV@mailbox.sc.edu

Supporting information and ORCID(s) from the author(s) for this article are available on the WWW under http://dx.doi.org/10.1002/anie.201508540.

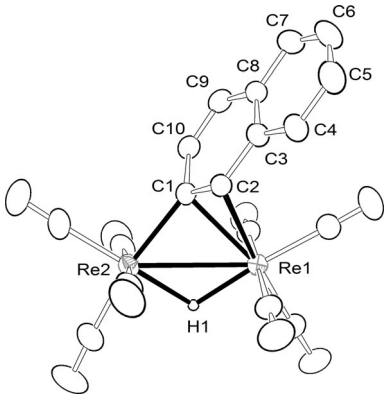

Figure 2. An ORTEP diagram of the molecular structure of $[Re_2(CO)_8(\mu\text{-}\eta^2\text{-}C_{10}H_7)(\mu\text{-}H)]$ (**3**). Thermal ellipsoids shown at 30% probability. Selected interatomic bond distances (Å) are as follows: Re1–Re2 = 3.0531(3) Å, Re1–C1 = 2.433(4), Re2–C1 = 2.196(4), Re1–C2 = 2.599(4), Re1–H1 = 1.83(5), Re2–H1 = 1.86(5), C1–C2 = 1.403(6).

In **3**, the naphthyl ligand serves as a three-electron donor, thus the rhenium atoms are formally electronically saturated and as a result, the Re–Re bond distance, 3.0531(3) Å, is significantly longer than that in the unsaturated **2**. A similarly coordinated $\mu\text{-}\eta^2$-naphthyl ligand was recently structurally characterized as one of two isomers of the triosmium complex $[Os_3(CO)_{10}(\mu\text{-}\eta^2\text{-}1,2\text{-}C_{10}H_7)][\mu\text{-}Au(PPh_3)]$.[7]

Most interestingly, it was found that **1** reacts with C_6D_6 to produce its deuterated equivalent $[D_6]$-**1** in quantitative yield within 11 hours at 60 °C [Equation (3)]. The same reaction yields $[D_6]$-**1** in 15% yield after 24 hours at 25 °C.

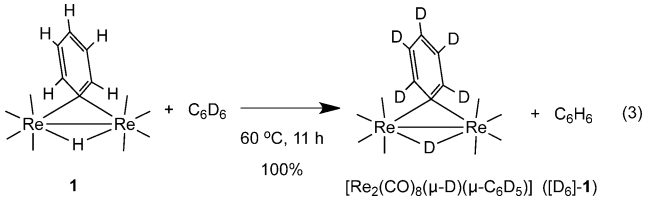

The mechanism of the aromatic C–H activation process by **1** was investigated by PBEsol-D3 geometry-optimized density-functional theory (DFT) calculations, performed in three steps as described in the Supporting Information. Not surprisingly, the initial stages of the process resemble that of the NCMe-induced elimination of benzene[6] from **1**. In both cases, the transformation is initiated by approach of an uncoordinated solvent molecule to **1** in the region proximate to its bridging hydride ligand (Scheme 1). The approaching solvent molecule donates some electron density from one of its π bonds to one of the rhenium atoms. A shift of the bridging phenyl ligand to a terminal position on the neighboring rhenium atom, via transition state **TS1**, yields the intermediate **I1**. In the present case, this intermediate is subsequently converted into an η^2-CH coordinated C_6H_6 ligand in the intermediate **I2** by a C–H bond-forming shift of the bridging hydrido ligand to the carbon atom of the terminally coordinated phenyl ligand via **TS2**. The intermediate **I2** subsequently rearranges into a centrosymmetrical bis$[\eta^2\text{-}(C,C)\text{-}C_6H_6]$ complex (**I3**) which is approximately 4 kcal mol^{-1} lower in energy than **I2** (Figure 3).

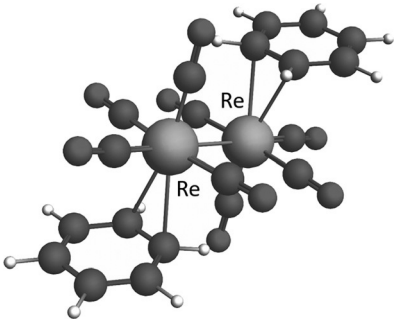

Figure 3. A computer-generated image of the DFT geometry-optimized structure of $[Re_2(CO)_8(\eta^2\text{-}C_6H_6)_2]$ (**I3**).

There are a number of examples of η^2-(C,C) arene complexes,[8,9] but there is evidence to show that aromatic C–H activations are preceded by the formation to η^2-C–H coordination at single metal sites.[4a,b,9] Pincer complexes containing aromatic η^2-(C,H) coordination have been isolated and are precursors to aromatic C–H activation.[10]

An energy level diagram of the reaction profile in Scheme 1 is shown in Figure 4. There are two transition states: **TS1** (+14.8 kcal) which involves the addition of the benzene molecule to **1**, and **TS2** (+16.0 kcal) which leads to the formation of the C–H bond in **I2**. In **I3** (+2.3 kcal), the two benzene ligands have become equivalent and either one could be used to regenerate **1** simply by reversing the process and expelling the remaining benzene ligand. The key step in the C–H activation process occurs in going from **I2** back to **I1**

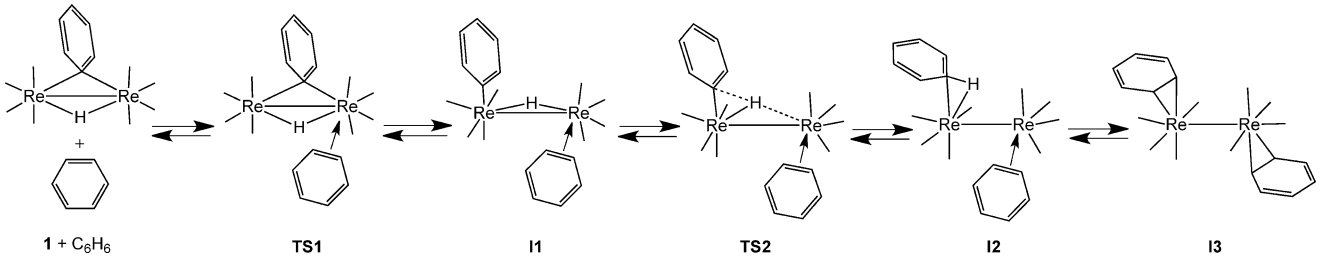

Scheme 1. C–H bond-forming and bond-cleavage processes involved in the benzene exchange reaction of **1**.

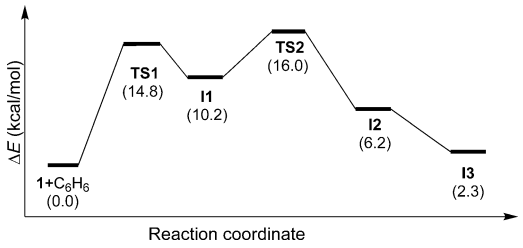

Figure 4. An energy profile of the transformations along the reaction coordinate during the exchange of C_6H_6 with **1**. The energies in kcal mol^{-1} are given within parentheses.

by microscopic reversibility via **TS2** or the inversion equivalent of **TS2** if the added benzene ligand is activated instead. The latter process would lead to benzene exchange and to [D_6]-**1** if the added benzene were C_6D_6. The C–H bond-breaking step begins at the rhenium atom, Re1, in **I2** (Scheme 1) where the benzene ligand is η^2-coordinated by a C–H bond. However, the calculations show that the second rhenium atom, Re2, assists in the cleavage step as represented in **TS2** by interacting with the hydrogen atom early in the cleavage process by facilitating its shift to its position as a bridge across the Re–Re bond. The C–H bond distance in **TS2** is 1.573 Å.

As established for the oxidative addition of H_2 to metal atoms,[11] the oxidative addition of C–H bonds to low-valent metal atoms can be viewed as a combination of two processes: 1) donation of electrons to a metal atom by utilizing the electrons in the C–H σ-bond, electrons which are ultimately used in the formation of metal–carbon and metal–hydrogen bonds; and 2) the cleavage of the C–H bond facilitated by the flow of electrons into the C–H σ*-bond.[3b,4a,12] Two MOs (the HOMO−7, −6.99 eV and the HOMO, −5.84 eV) presented in Figure 5 show the nature of the $Re_2(\eta^2$-CH) bonding in **TS2** at

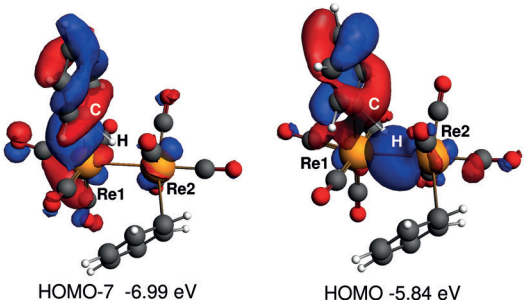

Figure 5. Two molecular orbitals, the HOMO−7 and HOMO, with calculated energy in eV for the transition state **TS2**. Shown is the nature of the bonding in the region of the important C–H bond during the C–H bond cleavage in the benzene ligand to form the phenyl and hydrido ligands at the two Re atoms in going from **I2** to **I1**. Re orange; isovalue = 0.03.

this critical stage of the transformation. The HOMO−7 shows the coordination of the C–H σ-bond to Re1 with the H atom directed toward Re2. The HOMO contains a node perpendicular to the η^2-C–H bond. This region of the molecular orbital can be viewed as the original antibonding σ*-orbital of C–H. Electron density in this molecular orbital is supplied to the C–H σ*-orbital, in a large part by electrons from the Re–Re bond, and facilitates the C–H bond cleavage process. The hydrogen atom in **TS2** is bonded both to Re1 and to Re2 wherein Re1–H is 1.785 Å and the Re2–H is 2.117 Å. In support of this proposal we also performed an ADF fragment analysis by dividing the refined structure of **TS2** into two fragments, one consisting of the activated C_6H_6 ligand, and one containing the remaining Re_2 portion of the molecule. It was found that the HOMO−7 of **TS2** consists of a combination of the HOMO of the activated C_6H_6 ligand and the LUMO of the Re_2 portion (Figure 6, left). The HOMO of **TS2**

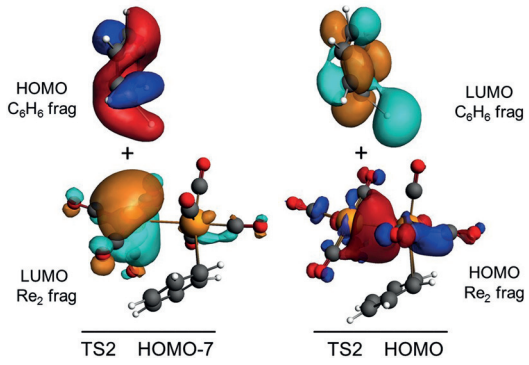

Figure 6. Molecular orbitals of the activated C_6H_6 fragment and the remaining Re_2 fragment of **TS2**. Left: the HOMO of C_6H_6 fragment and the LUMO of the Re_2 fragment are combined to form the HOMO−7 of **TS2**; isovalue = 0.03. Right: LUMO of C_6H_6 fragment and the HOMO of the Re_2 fragment are combined to form the HOMO of **TS2**; isovalue = 0.03.

was found to consist of principally of the LUMO of the activated C_6H_6 ligand and the HOMO of the Re_2 group, the latter is dominated by the Re–Re bond (Figure 6, right).

In summary, the calculations demonstrate a clear binuclear metal character in the C–H bond-cleavage step in benzene at its most critical point. One can imagine similar processes leading to the formation of **1** and **2**. In this study we have shown that a binuclear Re_2 unit is very effective for aromatic C–H oxidative additions and both metal atoms are involved in the C–H bond-cleavage process, which occurs, albeit slowly, even at room temperature. The facile activation of aromatic C–H bonds in this new system may pave the way for the development of binuclear hydroarylation reactions and other types of aromatic functionalization reactions.[13,14] These results also may have implications for the nature of C–H bond-cleavage processes at polynuclear metal sites on metal nanoparticles[15] and on metal surfaces.[16]

Experimental Section

Synthesis of **2**: 20 μL (0.1250 mmol) of *N*,*N*-diethylaniline was added to 30.0 mg (0.0444 mmol) of **1** dissolved in 2 mL of CD_2Cl_2 and stirred at 50 °C for 5.5 h. A brown solution was formed and the solvent was then removed in vacuo. The residue was extracted in methylene chloride and separated by thin layer chromatography to provide pure yellow **2** in 61 % yield.

Synthesis of **3**: 10.0 mg (0.0780 mmol) of naphthalene ($C_{10}H_8$) was added to 20.0 mg (0.0296 mmol) of **1** dissolved in 5 mL of methylene chloride and stirred at 50 °C for 15 h. A light yellow solution was formed and the solvent was then removed in vacuo. The residue was extracted in methylene chloride and separated by thin layer chromatography to provide pure yellow **3** in 44 % yield.

The formation of [D_6]-**1** was performed by dissolving **1** in pure C_6D_6 in an NMR tube and heating to 60 °C for a period of 11 h. A mass spectrum of the **1** after this period showed it was converted to [D_6]-**1** in 100 % amount. The same reaction yields [D_6]-**1** in 15 % yield after 24 h at 25 °C.

Single-crystal structure determination: The intensity data were collected by using a Bruker SMART APEX CCD-based diffractometer with Mo Kα radiation ($\lambda = 0.71073$ Å) at 294 K. All non-hydrogen atoms were refined with anisotropic thermal parameters. Hydrogen atoms were placed in geometrically idealized positions and included as standard riding atoms during the least-square refinements.

Crystal data for **2**: $Re_2O_8NC_{18}H_{15}$, monoclinic, $P21/n$, $M_r = 745.71\ g\,mol^{-1}$, $a = 12.4057(14)$, $b = 11.9489(14)$, $c = 14.8370(17)$ Å, $\alpha = 90.00$, $\beta = 97.005(2)$, $\gamma = 90.00°$, $V = 2182.9(4)$ Å^3, $Z = 4$, $\rho_{calcd} = 2.269\ g\,cm^{-3}$, $\mu = 11.122\ mm^{-1}$; $2\theta_{max} = 56.06°$, $F(000) = 1376$, $R_{int} = 0.0424$, no. collected/unique/$I_0 > 2\sigma I_0$ data = 22663/3865/3204, R1/wR2(all data) = 0.0286/0.0506, R1/wR2($I_0 > 2\sigma I_0$) = 0.0214/0.0470), max./min. electron density = 1.017/−0.441 e$^-$ Å^{-3}.

Crystal data for **3**: $Re_2O_8C_{18}H_8$, triclinic, $P\bar{1}$, $M_r = 724.64\ g\,mol^{-1}$, $a = 8.6200(4)$, $b = 9.7881(5)$, $c = 13.4320(6)$ Å, $\alpha = 96.321(1)$, $\beta = 107.737(1)$, $\gamma = 113.108(1)°$, $V = 958.10(8)$ Å^3, $Z = 2$, $\rho_{calcd} = 2.512\ g\,cm^{-3}$, $\mu = 12.665\ mm^{-1}$, $2\theta_{max} = 56.52°$, $F(000) = 660$, $R_{int} = 0.0307$, no. collected/unique/$I_0 > 2\sigma I_0$ data = 10321/3385/3074, R1/wR2(all data) = 0.0251/0.0560, R1/wR2($I_0 > 2\sigma I_0$) = 0.0220/0.0541), max./min. electron density = 0.752/−1.112 e$^-$ Å^{-3}.

CCDC 1422546 (**2**) and 1422547 (**3**) contain the supplementary crystallographic data for this paper. These data can be obtained free of charge from The Cambridge Crystallographic Data Centre.

Acknowledgments

This research was supported by the following grants from the National Science Foundation: CHE-1111496 and CHE-1464596, with computations performed on the computer cluster supported by CHE-1048629.

Keywords: bridging ligands · C–H activation · density-functional calculations · rhenium · structure elucidation

How to cite: *Angew. Chem. Int. Ed.* **2016**, *55*, 1324–1327
Angew. Chem. **2016**, *128*, 1346–1349

[1] A. E. Shilov, G. B. Shul'pin, *Activation and Catalytic Reactions of Saturated Hydrocarbons in the Presence of Metal Complexes*, Kluwer Academic Pub., New York, **2002**.

[2] a) M. Sun, J. Zhang, P. Putaj, V. Caps, F. Lefebvre, J. Pelletier, J.-M. Basset, *Chem. Rev.* **2014**, *114*, 981–1019; b) R. G. Bergman, *Nature* **2007**, *446*, 391–393; c) A. E. Shilov, G. B. Shul'pin, *Chem. Rev.* **1997**, *97*, 2879–2932; d) A. Caballero, P. J. Pérez, *Chem. Soc. Rev.* **2013**, *42*, 8809–8820; e) A. Gunay, K. H. Theopold, *Chem. Rev.* **2010**, *110*, 1060–1081; f) R. H. Crabtree, *J. Organomet. Chem.* **2004**, *689*, 4083–4091; g) J. R. Webb, T. BolaÇo, T. B. Gunnoe, *ChemSusChem* **2011**, *4*, 37–49.

[3] a) J. A. Labinger, J. E. Bercaw, *Nature* **2002**, *417*, 507–514; b) D. Balcells, E. Clot, O. Eisenstein, *Chem. Rev.* **2010**, *110*, 749–823.

[4] a) M. Lersch, M. Tilset, *Chem. Rev.* **2005**, *105*, 2471–2526; b) C. Hall, R. N. Perutz, *Chem. Rev.* **1996**, *96*, 3125–3146; c) W. D. Jones, *Acc. Chem. Res.* **2003**, *36*, 140–146; d) E. S. Rudakov, G. B. Shul'pin, *J. Organomet. Chem.* **2015**, *793*, 4–16; e) J. A. Labinger, J. E. Bercaw, *J. Organomet. Chem.* **2015**, *793*, 47–53.

[5] a) W. D. McGhee, F. J. Hollander, R. G. Bergman, *J. Am. Chem. Soc.* **1988**, *110*, 8428–8443; b) K. Fujita, Y. Takahashi, H. Nakaguma, T. Hamada, R. Yamaguchi, *J. Organomet. Chem.* **2008**, *693*, 3375–3382; c) R. J. Goudsmit, B. F. G. Johnson, J. Lewis, P. R. Raithby, M. J. Rosales, *J. Chem. Soc. Dalton Trans.* **1983**, 2257–2261; d) T. Takao, M. Moriya, M. Kajigaya, H. Suzuki, *Organometallics* **2010**, *29*, 4770–4773.

[6] R. D. Adams, V. Rassolov, Y. O. Wong, *Angew. Chem. Int. Ed.* **2014**, *53*, 11006–11009; *Angew. Chem.* **2014**, *126*, 11186–11189.

[7] R. D. Adams, V. Rassolov, Q. Zhang, *Organometallics* **2013**, *32*, 6368–6378.

[8] a) W. D. Jones, F. Feher, *Acc. Chem. Res.* **1989**, *22*, 91–100; b) C. L. Higgitt, A. H. Klahn, M. H. Moore, B, Oelckers, M. G. Partridge, R. N. Perutz, *J. Chem. Soc. Dalton Trans.* **1997**, 1269–1280; c) W. D. Jones, L. Dong, *J. Am. Chem. Soc.* **1989**, *111*, 8722–8723; d) W. D. Harman, *Chem. Rev.* **1997**, *97*, 1953–1978; e) C. D. Tagge, R. G. Bergman, *J. Am. Chem. Soc.* **1996**, *118*, 6908–6915; f) A. Stanger, R. Boese, *J. Organomet. Chem.* **1992**, *430*, 235–243; g) D. J. Brauer, C. Krueger, *Inorg. Chem.* **1977**, *16*, 884–891.

[9] a) Z. E. Clot, B. Oelckers, A. H. Klahn, O. Eisenstein, R. N. Perutz, *Dalton Trans.* **2003**, 4065–4074; b) M. Lavin, E. M. Holt, R. H. Crabtree, *Organometallics* **1989**, *8*, 99–104; c) A. C. Albéniz, G. Schulte, R. H. Crabtree, *Organometallics* **1992**, *11*, 242–249; d) D. G. Churchill, K. E. Janak, J. S. Wittenberg, G. Parkin, *J. Am. Chem. Soc.* **2003**, *125*, 1403–1420.

[10] a) A. Vigalok, O. Uzan, L. J. W. Shimon, Y. Ben-David, J. M. L. Martin, D. Milstein, *J. Am. Chem. Soc.* **1998**, *120*, 12539–12544; b) P. Dani, T. Karlen, R. A. Gossage, W. J. J. Smeets, A. L. Spek, G. van Koten, *J. Am. Chem. Soc.* **1997**, *119*, 11317–11318.

[11] G. J. Kubas, *Metal Dihydrogen and Sigma Bond Complexes*, Kluwer, New York, **2002**, pp. 365–411.

[12] J.-Y. Saillard, R. Hoffmann, *J. Am. Chem. Soc.* **1984**, *106*, 2006–2026.

[13] a) F. Kakiuchi, S. Murai, *Acc. Chem. Res.* **2002**, *35*, 826; b) N. A. Foley, J. P. Lee, Z. Ke, T. B. Gunnoe, T. R. Cundari, *Acc. Chem. Res.* **2009**, *42*, 585–597; c) J. Oxgaard, R. A. Periana, W. A. Goddard III, *J. Am. Chem. Soc.* **2004**, *126*, 11658–11665.

[14] a) K. Gao, N. Yoshikai, *Acc. Chem. Res.* **2014**, *47*, 1208–1219; b) M. S. Khan, A. Haque, M. K. Al-Suti, P. R. Raithby, *J. Organomet. Chem.* **2015**, *793*, 114–133; c) D. A. Colby, R. G. Bergman, J. A. Ellman, *Chem. Rev.* **2010**, *110*, 624–655; d) J. R. Andreatta, B. A. McKeown, T. B. Gunnoe, *J. Organomet. Chem.* **2011**, *696*, 305–315; e) B. A. Vaughan, M. S. Webster-Gardiner, T. R. Cundari, T. B. Gunnoe, *Science* **2015**, *348*, 421–424.

[15] a) F. Viñes, Y. Lykhach, T. Staudt, M. P. A. Lorenz, C. Papp, H.-P. Steinrück, J. Libuda, K. M. Neyman, A. Görling, *Chem. Eur. J.* **2010**, *16*, 6530–6539; b) Y.-H. Chin, C. Buda, M. Neurock, E. Iglesia, *J. Am. Chem. Soc.* **2011**, *133*, 15958–15978; c) Y.-H. Chin, C. Buda, M. Neurock, E. Iglesia, *J. Am. Chem. Soc.* **2013**, *135*, 15425–15442.

[16] a) E. S. Kryachko, A. V. Arbuznikov, M. F. A. Hendrickx, *J. Phys. Chem. B* **2001**, *105*, 3557–3566; b) M. Saeys, M.-F. Reyniers, M. Neurock, G. B. Marin, *J. Phys. Chem. B* **2003**, *107*, 3844–3855.

Received: September 11, 2015
Published online: December 8, 2015

